Journal of Marine Research, 41, 487–510, 1983

Exploratory observations of abyssal currents in the South Atlantic near Vema Channel

by William J. Schmitz, Jr.[1] and Nelson G. Hogg[1]

ABSTRACT

Vema Channel (nominal location 30S, 40W) is a major passage for the flow of Antarctic Bottom Water on its way northward from the Argentine Basin to the Brazil Basin. New data based on approximately year-long current meter deployments at abyssal depths yield mean or time-averaged kinetic energies as strong as 240 cm^2s^{-2}, and eddy kinetic energies from 8 to 40 cm^2s^{-2}. We observe a persistent northward flow of AABW with maximum speed near 40 cm s^{-1}, as is found at abyssal depths in the vicinity of the Gulf Stream. The highest value of mean kinetic energy in Vema Channel (240 $cm^2 s^{-2}$) is much larger than that (~20 $cm^2 s^{-2}$) found in the flow of Antarctic Bottom Water near the Ceara Rise, and comparable to values of 220 $cm^2 s^{-2}$ for the southward flow of North Atlantic Deep Water on the Blake-Bahama Outer Ridge. Existing observations of mean kinetic energy at locations near the Gulf Stream System do not exceed 100 $cm^2 s^{-2}$ in the abyssal depth range.

Eddy kinetic energies of 8 $cm^{-2} s^{-2}$ are comparable to estimates (at similar depths) from areas at roughly equivalent latitudes, like MODE (*M*id-*O*cean *D*ynamics *E*xperiment, nominal location 28N, 70W). However, abyssal kinetic energies as large as 40 $cm^2 s^{-2}$ are normally found only near strong current regimes, in contrast to values of roughly 1 $cm^2 s^{-2}$ in the ocean interior. Values of 18 to 64 $cm^2 s^{-2}$ have been observed near the southward flow of North Atlantic Deep Water on and adjacent to the Blake-Bahama Outer Ridge near 30N, and up to 20 $cm^2 s^{-2}$ in the flow of Antarctic Bottom Water over the Ceara Rise. The strongest abyssal eddy field yet observed, ~100 to 150 $cm^2 s^{-2}$, occurs near the Gulf Stream.

1. Introduction

During 1979 and 1980, a joint geological and physical oceanographic field program was carried out in the vicinity (Fig. 1) of Vema Channel. The new data base acquired included approximately 100 CTD stations, with five mooring sites occupied for somewhat longer than one year. The primary physical oceanographic objective was description and rationalization (Hogg *et al.*, 1982; Hogg, 1983b) of the flow of Antarctic Bottom Water (AABW) through the channel. An auxiliary goal was to characterize the time-averaged properties of the moored instrument data; our main objective in this note. Short-term (few week duration) current meter data in the vicinity of Vema Channel (Johnson *et al.*, 1976; Reid *et al.*, 1977) were obtained previously, but to the best of our knowledge we are considering the first exploratory

1. Woods Hole Oceanographic Institution, Woods Hole, Massachusetts, 02543, U.S.A.

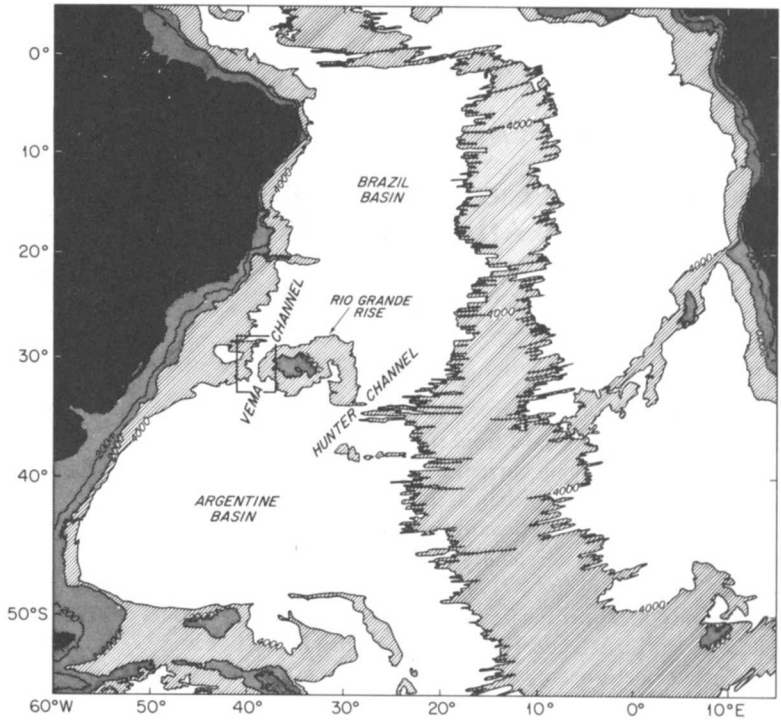

Figure 1. Basin geography, and bathymetry surrounding the observational area, the latter indicated by a rectangle superimposed over a region containing Vema Channel. This is a modified version of Figure 1 by Hogg *et al.* (1982). Details of the topography within the rectangle surrounding Vema Channel are contained in Figure 2.

data of significant duration, restricted to abyssal depths by the vagaries of fortune, from anywhere near the part of the South Atlantic Ocean under consideration.

The Rio Grande Rise (Fig. 1), oriented zonally along roughly 30S from the coast of South America to the mid-Atlantic Ridge, forms a barrier between the Argentine and Brazil Basins (at the southern end of the latter). There are two main abyssal passages through the Rio Grande Rise, called Vema and Hunter Channels (Johnson *et al.*, 1976). The sill depth of Hunter Channel according to Johnson *et al.* (1976) is several hundred meters shallower than that of Vema Channel, the latter being the principal passage for the northward flow of AABW. In Figure 1, Vema Channel is surrounded by a 4 × 6 degree region whose depth contours are contained in Figure 2a. Figure 2b depicts the local bathymetry surrounding the moored instrument array on a 1 × 1 degree grid. The axis of Vema Channel may be visualized in Figures 2a and 2b as a conduit between the 4500 m depth contours, oriented approximately north-south (near the center of the figure). The mooring array was set across this passage (mooring sites 1 to 4), with one other mooring site (5) chosen to be approximately along the axis of the channel, "downstream" from the mooring transect relative to the expected flow of

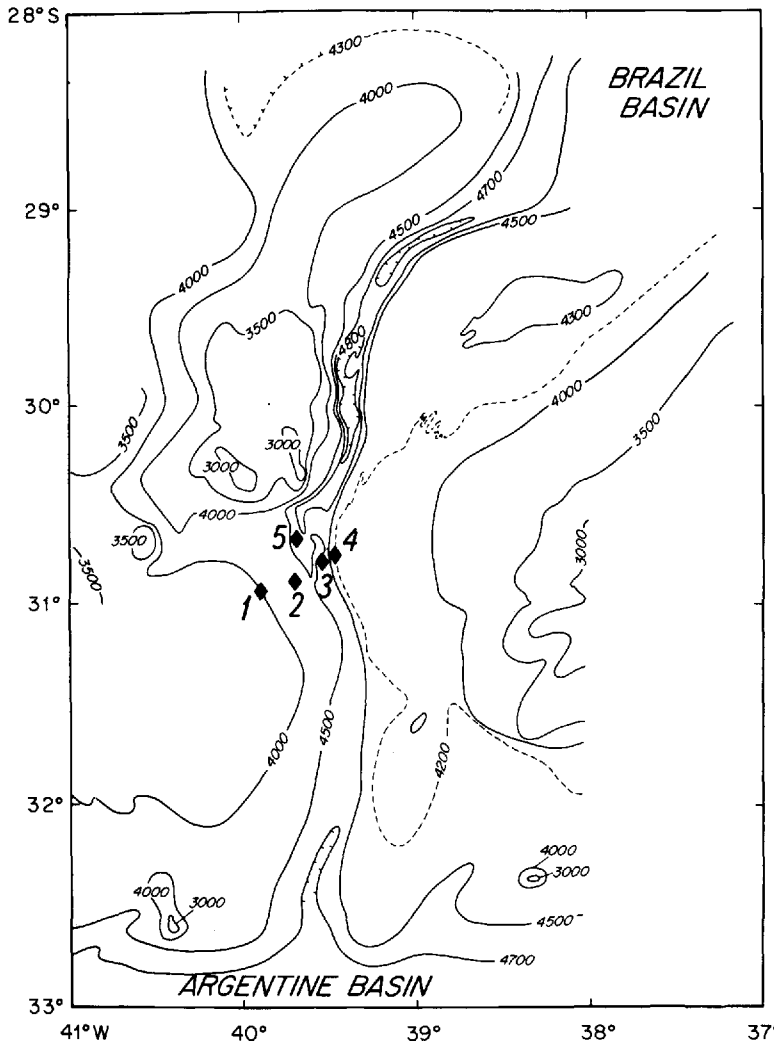

Figure 2. Depth contours near Vema Channel: (a) For the region denoted by the rectangle in Figure 1. Mooring sites are superimposed (solid diamonds numbered 1 through 5). This is a modified version of Figure 2 by Hogg *et al.* (1982). Depth contours in meters. (b) In the vicinity of the mooring sites, denoted by open circles containing numbers 1 through 5. Bathymetry adapted from Johnson (1982, personal communication). Depth contours in hundreds of meters.

AABW (mooring site locations are superimposed on Fig. 2). The strongest currents, mean and fluctuating, are found at mooring site 3.

The position of the observational area around Vema Channel with respect to the distribution of the intensity of eddy and mean fields at the sea surface (according to Wyrtki *et al.*, 1976) is illustrated in Figures 3a and 3b respectively. Vema Channel is

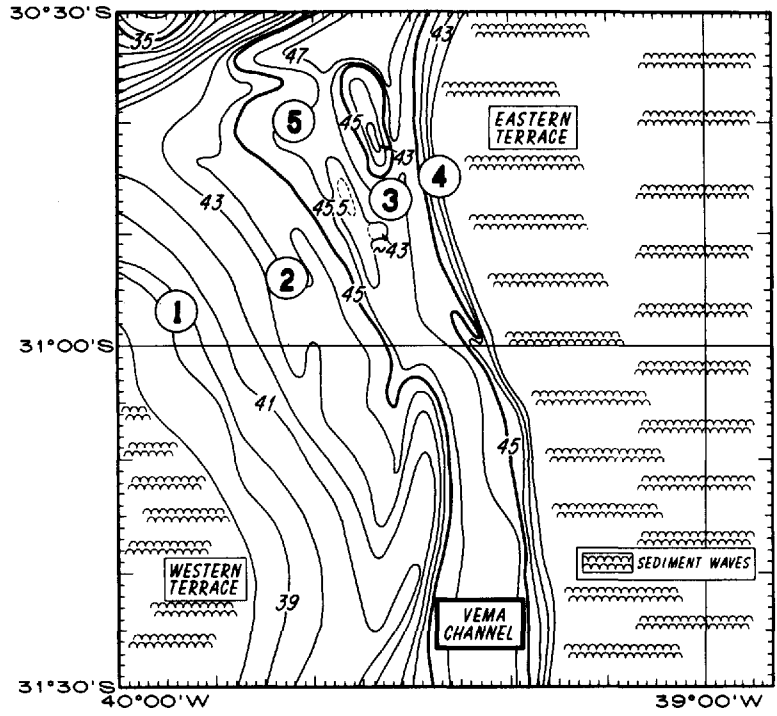

Figure 2. Continued.

situated in a region that is approximately equivalent to MODE (*M*id-*O*cean *D*ynamics *E*xperiment, nominal location 28N, 70W) or LDE (*L*ocal *D*ynamics *E*xperiment, nominal location 31N, 70W) in terms of relative location in a subtropical gyre circulation as well as geographically (except that Vema Channel is somewhat closer to a coastline). However, the essential geographical point of comparison is probably location relative to abyssal or thermohaline flow patterns. Both AABW and NADW form deep or abyssal western boundary currents that traverse the (subtropical gyre) latitudes of the data-sets being considered. The AABW current regime in Vema Channel is analogous to the flow of North Atlantic Deep Water (NADW) at similar latitudes along the Blake-Bahama Outer Ridge (Mills and Rhines, 1979; Jenkins and Rhines, 1980). We will follow Hogg (1983a) in calling the latter flow regime the DWBC (*D*eep *W*estern *B*oundary *C*urrent).

Basic properties of the data are described and discussed in Section 2, after which pertinent characteristics of the Vema Channel observations are outlined (Section 3). A comparison with data from other locations in Section 4 is followed by summary and conclusions (Section 5).

2. The data base

Cruises to Vema Channel were made in the fall of 1979 and spring of 1980 and 1981: moorings were set on the first and recovered on the latter pair. Details of mooring

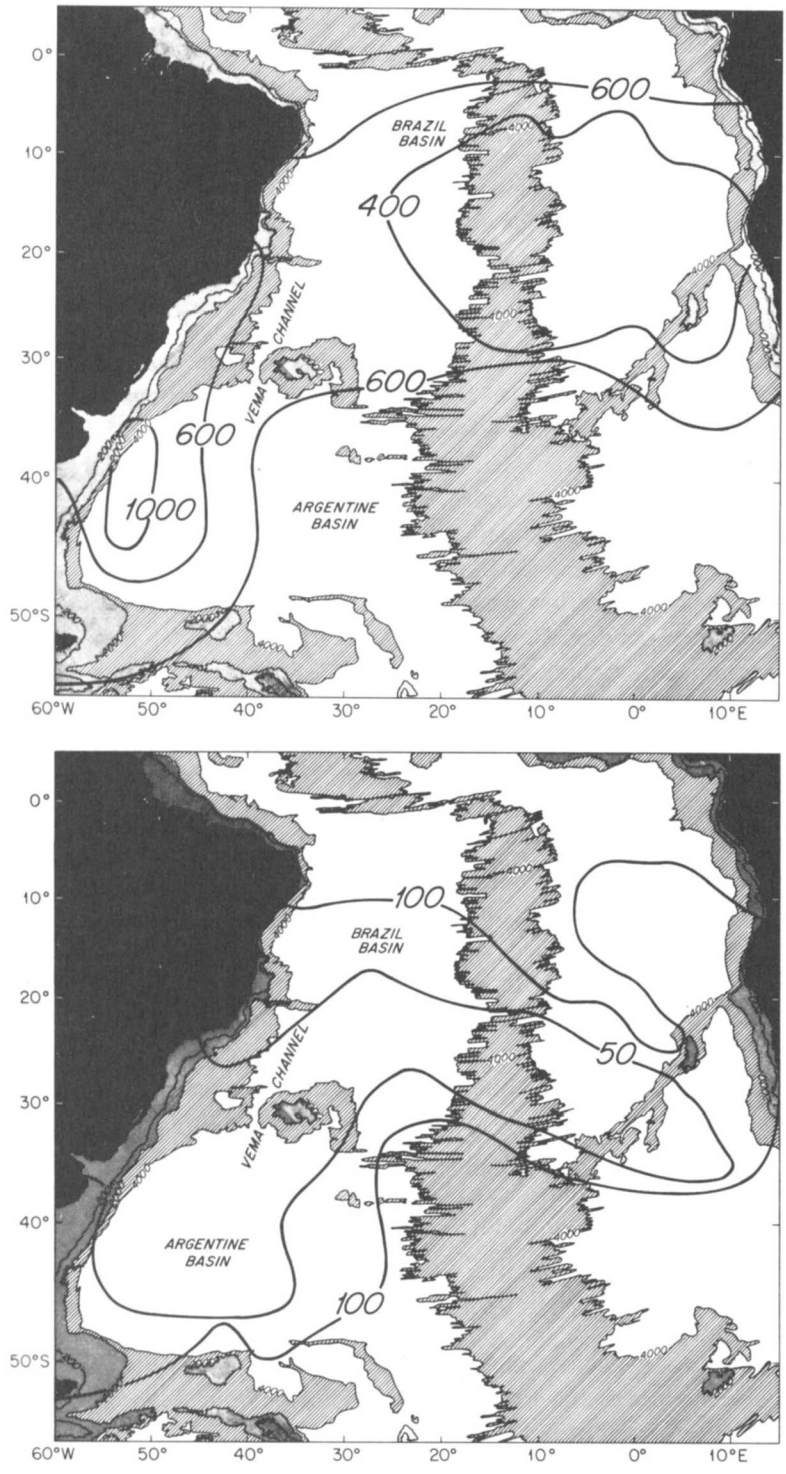

Figure 3. A map of the South Atlantic (similar to Fig. 1) with selected contours (adapted from Wyrtki *et al.*, 1976) superimposed: (a) of surface eddy kinetic energy ($cm^2\ s^{-2}$); (b) of surface mean kinetic energy ($cm^2\ s^{-2}$).

design and data acquisition have been described by Hogg *et al.* (1982); five mooring sites (numbered 1 through 5 in Figure 2 and in the following) were chosen. Table 1 in Hogg *et al.* (1982) contains extensive logistical detail concerning mooring and instrument configuration. The moorings were deployed twice due to battery problems; first for a few months, then for about a year. Each mooring is assigned a number sequentially as deployed by the buoy group at the Woods Hole Oceanographic Institution. Instruments are then identified by adding a digit to the end of the mooring number, starting from the top of the mooring. For example, 6891 is the shallowest instrument (1) on mooring 689. Mooring numbers for the first array setting were 681–685 and correspondingly 688–692 for the second deployment. A simplified moored array is shown in Figure 4 [see also Figure 3 in Hogg *et al.* (1982)].

Upon (each) recovery from sea, magnetic tape cassettes were extracted from the current-temperature meters, decoded, and placed in computer-compatible form [see Fig. 4 for hardware identification, and other publications, for example, Gould *et al.* (1974) for an instrumental discussion]. Each record was taken through standard quality control procedures, low-passed with the filter described by Schmitz (1974), and sub-sampled once per day. Various time averages and Fourier transforms are then routinely computed. Schmitz and Hogg (1978) describe similar data handling procedures for an analogous data set; see also Mills and Rhines (1979). The zonal and meridional (x, y) means and variances are denoted by $(\overline{u}, \overline{v})$ and $(\overline{u'^2}, \overline{v'^2})$; the overbar signifies a time average (over the record length), and a prime superscript indicates deviation from that average. Eddy kinetic energy (per unit mass, hereafter understood) is $K_E = .5\ (\overline{u'^2} + \overline{v'^2})$, and (K_u, K_v) are zonal and meridional eddy kinetic energies. Mean kinetic energy is $K_M = .5\ (\overline{u}^2 + \overline{v}^2)$, $(\overline{K}_u, \overline{K}_v)$ are zonal and meridional mean kinetic energies. In this context then, "eddies" are not necessarily closed circulation cells or any explicitly defined spatial entity, but encompass all low frequency variability about the mean, with periods longer than the filter (or sampling) cut-off (around 2 days), and shorter than periods covered by the mean (twice the record length and longer by definition). In calculating eddy energies, the inverse of the low-pass filter initially used is applied at frequencies lower than .5 cycle per day, a matter of consequence primarily for periods of a few days (slightly above the filter cut-off). This consideration is rarely significant at mid-latitudes (it is not for Vema Channel), but is important for the low-latitude Ceara Rise data discussed below.

The Fourier transform procedure employed assigns energy to each of the basic frequency bands $(\alpha \pm .5)\ \tau^{-1}$, where τ is the record length and $\alpha = 1, \ldots N - 1$; N is one-half the number of data days. The highest frequency $(\alpha = N)$ is a cycle per two days and encompasses only half the bandwidth of the lower frequency estimates, as does the mean $(\alpha = 0)$, which spans the frequency band from zero to $(2\tau)^{-1}$. The lowest frequency band above the mean contains contributions from the range of periods from $(2/3 \rightarrow 2)\ \tau$, "centered" at τ.

A variety of techniques for presenting frequency distributions may be used, depending on what one wants to emphasize. We use the summed energy in a few rather

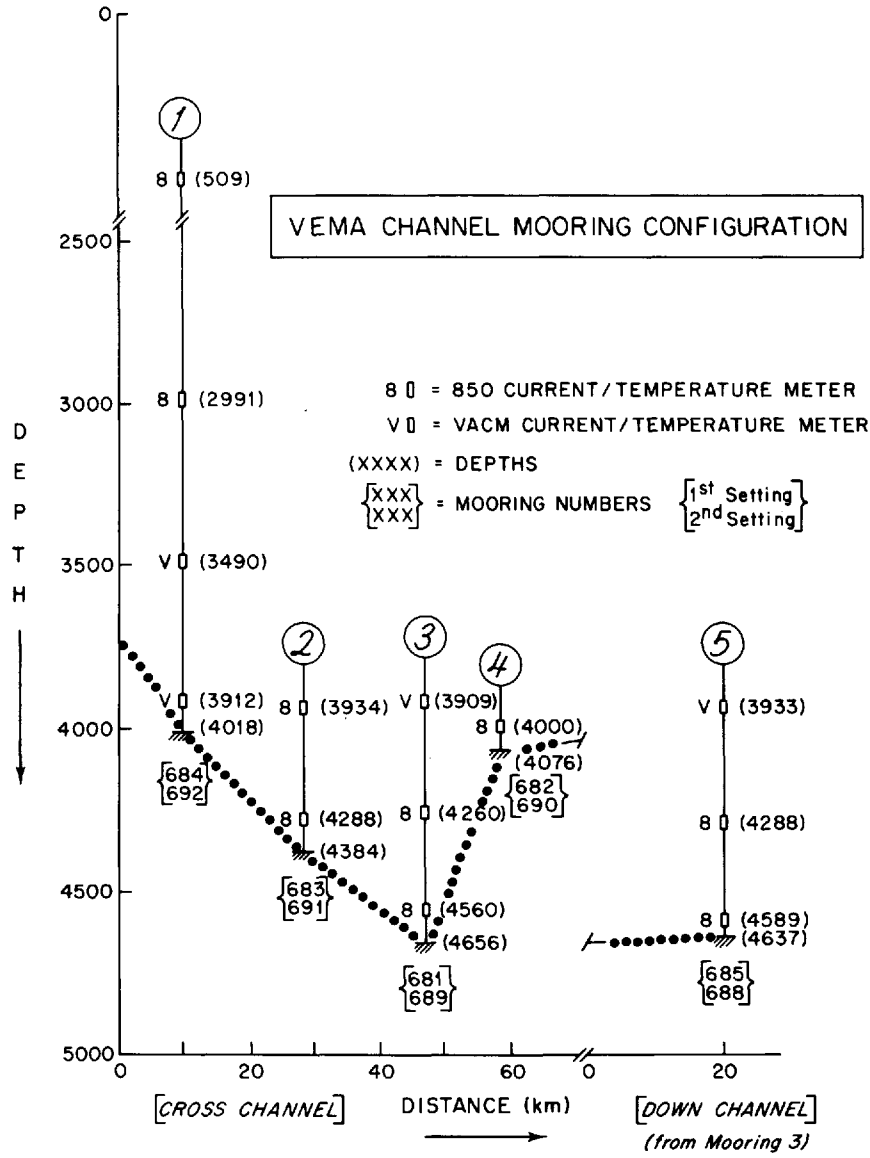

Figure 4. A section across the Vema Channel array: the instrument depths for sites 1 through 5 are for the second mooring deployment. The dotted line and hatched symbols denote bottom depths. This is a condensed and modified version of Figure 3 by Hogg *et al.* (1982).

broad frequency bands or period ranges as our basic time scale description: the notation K_E (a, b) will be used to designate the eddy kinetic energy in the range of periods from a to b days (or the frequency band b^{-1} to a^{-1} cycles per day). The "eddy band" has been taken to encompass periods from 20–40 to 100–300 days. Here we use 20 to 100 or 40 to 100, nominal, with shorter periods simply called "the high

Table 1. Vema Channel mooring (second setting) locations, dates and deployment times.

Site #	Mooring #	Latitude Longitude	Bottom depth (m)	Date set	Duration (days)
1	692	30° 56.1'S 39° 53.6'W	4018	Mar. 26, 1980	354
2	691	30° 53.5'S 39° 41.7'W	4384	Mar. 25, 1980	No rotor after 8–9 days
3	689	30° 47.1'S 39° 32.0'W	4656	Mar. 24, 1980	356
4	690	30° 45.2'S 39° 27.6'W	4076	Mar. 25, 1980	356
5	688	30° 39.9'S 39° 49.0'W	4637	Mar. 23, 1980	358

frequencies." Periods longer than 100 days or so, but shorter than twice the record length, are referred to as "secular scale." Coherence is the magnitude of the vector having co- and quadrature spectral estimates as components.

Instrument performance generally speaking was poor, and several sites where data are available for the first setting did not have working instruments for the second. Results from the second array setting (Table 1) constitute the primary data base used in the following, since we are primarily interested in long-term averages. There are eight high-quality records of about one-year duration (second setting) and six high quality merged (first and second setting) files of approximately 450-day duration.

Basic time averages for the long-term records are listed in Tables 2 and 3. Calculation over a common time applies to all quantities where a significant problem could arise otherwise. Averages pertaining to the eddy field in Tables 2 and 3 (with one exception) are for records of identical start date and duration (a common 350 days for records from the second setting and 450 days for the combined or merged files). However, the averages pertaining to the mean fields in Table 2 were taken over the (maximum) deployment times indicated in Table 1; intervals of up to 358 days. Similar quantities in Table 3 were taken over 451–467 days depending on mooring site.

Table 2. Depths and basic time averages for the long-term (350 days or longer) data obtained on the moorings noted in Table 1.

Site #	Rec. #	Depth (m)	$\bar{u}$ (cm s^{-1})	$\bar{v}$ (cm s^{-1})	K_M (cm^2 s^{-2})	K_u (cm^2 s^{-2})	K_v (cm^2 s^{-2})	K_E (cm^2 s^{-2})
1	6924	3912	−3.4	9.6	51.9	3.0	10.4	13.4
3	6891	3909	−2.0	6.4	22.5	6.2	21.4	27.6
3	6893	4260	−2.0	21.7	237.4	2.3	36.8	39.1
3	6894	4560	−3.3	21.7	240.8	4.1	28.1	32.2
4	6901	4000	−.9	−1.9	2.2	5.5	10.8	16.3
5	6881	3933	2.2	8.9	42.0	2.7	13.8	16.5
5	6882	4288	2.1	12.8	84.1	1.5	10.5	12.0
5	6883	4589	.5	11.8	69.7	.8	7.3	8.1

Table 3. Depths and basic time averages for merged (first and second settings) moored instrument records; durations are 451 to 468 days. Positions and bottom depths essentially as in Table 1.

Site #	Rec. #	Depth (m)	$\bar{u}$ (cm s^{-1})	$\bar{v}$ (cm s^{-1})	K_M (cm^2 s^{-2})	K_u (cm^2 s^{-2})	K_v (cm^2 s^{-2})	K_E (cm^2 s^{-2})
1	6844, 6924	3911, 3912	−3.3	9.7	52.5	2.6	11.2	13.8
3	6811, 6891	3925, 3909	−2.2	7.0	26.9	6.5	19.1	25.6
3	6813, 6893	4275, 4260	−2.4	21.8	240.5	3.1	35.4	38.5
5	6851, 6881	3971, 3933	2.1	9.2	44.5	3.5	12.9	16.4
5*	6852, 6882	4326, 4288	2.1	12.9	85.4	1.6	9.6	11.2
5	6853, 6883	4627, 4589	0.6	11.6	67.5	.9	7.4	8.3

*Time-dependent stats computed over 467 days.

We will primarily use the eight-record observational base associated with the second mooring deployment, as opposed to six-record merged data set, since dissimilarities in behavior associated with the differences between 350 and 450 day duration are not significant for our purposes. The maximum relative difference between these two data sets in K_E (taken from Table 3) is 8%, for the topmost instrument at site 3 (6891 vs. 6811 + 6891). A frequency distribution for this intercomparison is contained in Table 4. Most of the difference between 6891 vs. 6811 + 6891 is contained in the lowest frequency band. For another example (6813 + 6893 vs. 6893) however, also listed in Table 4, there are noticeable differences at the higher frequencies as well. Consistencies between settings have in fact been used as a quality control technique; specifically, an error in 6852 (relative to Hogg *et al.*, 1982) was initially located this way.

Table 4. A comparison of the frequency distribution of K_E for records of different duration at the same location in Vema Channel. Period ranges for different records are dissimilar, as indicated in columns at each side of the Table.

Period ranges merged files (days)		K_E (6811 + 6891)	K_E (6891)	K_E (6813 + 6893)	K_E (6893)	Period ranges 2nd setting (days)	
T_1	T_2	(cm^2 s^{-2})	(cm^2 s^{-2})	(cm^2 s^{-2})	(cm^2 s^{-2})	T_1	T_2
2	20	5.6	5.5	7.3	8.1	2	20
20	42.9	3.0	2.8	9.7	8.7	20	41.2
42.9	100	6.7	7.2	9.5	8.6	41.2	100
100	900	10.3	12.1	12.0	13.7	100	700
Totals →		25.6	27.6	38.5	39.1	← Totals	

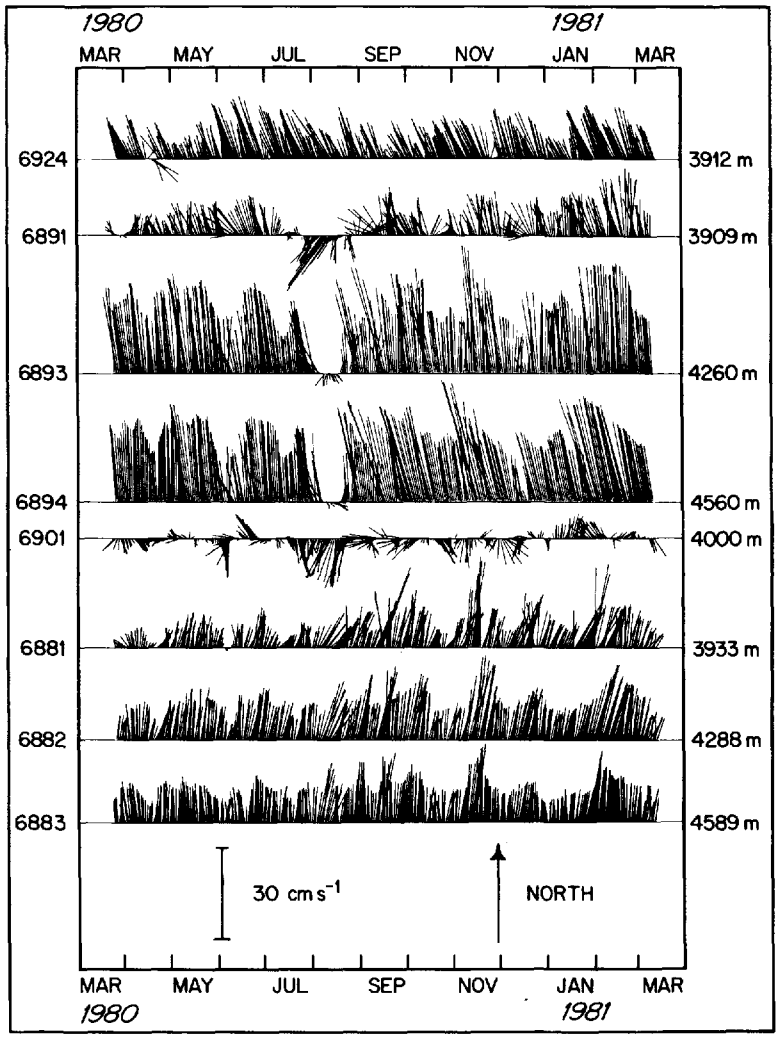

Figure 5. Time series of horizontal velocity vectors (record number in left margin, depths in right-hand margin): (a) for the (eight) nearly year-long Vema Channel records; (b) for the (eleven) long-term records in the vicinity of the Deep Western Boundary Current along the Blake-Bahama Outer Ridge.

As indicated in Figure 4, instruments at site 1 were set in the thermocline and at "intermediate depths" as well as an abyssal level. Unfortunately, the thermocline instruments failed on both deployments, in spite of discovering the first failure and replacing it with a different meter for the second mooring launch. In addition, the (site 1) instruments at intermediate depths (3000 and 3500 m, nominal) had serious performance problems during the second setting. Therefore, there are no (high-quality) long-term moored instrument data from depths of 3500 m or less. The top of

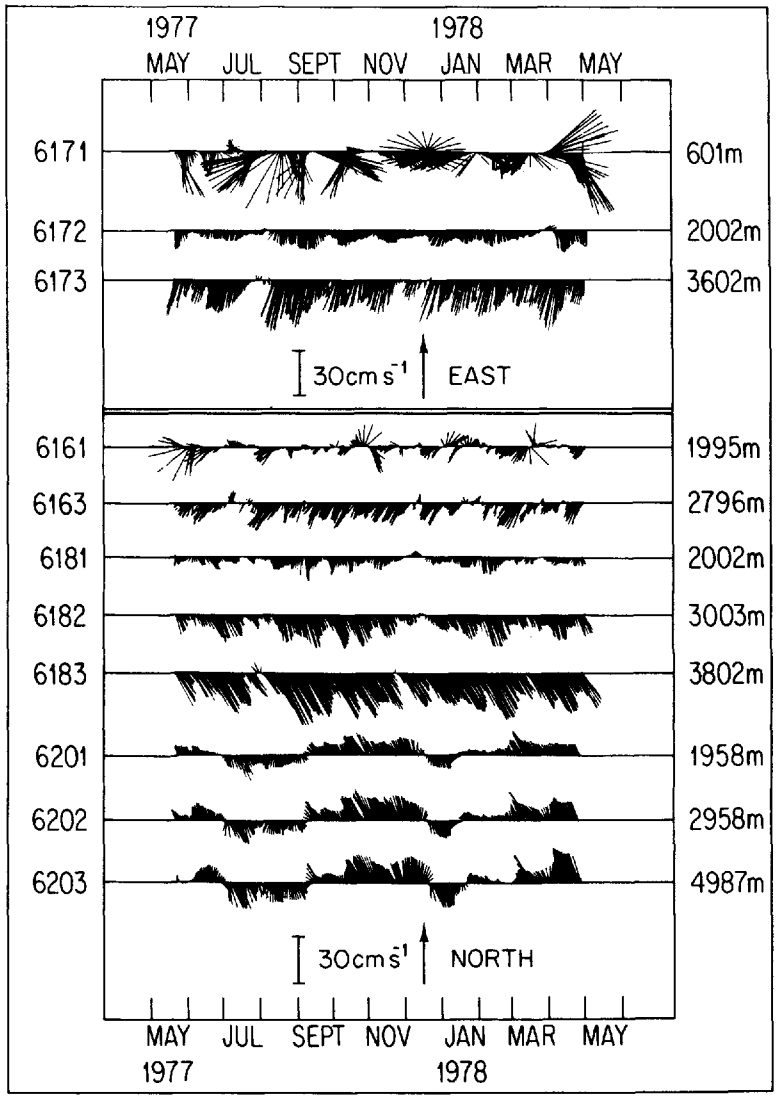

Figure 5. Continued.

the Rio Grande Rise to the west of Vema Channel (often called the Sao Paulo Plateau now), is at about 3700 m excepting small scale features (Fig. 2), roughly the transition depth from AABW to NADW. As a result, the following discussion is restricted to AABW at abyssal depths, in or near the AABW flow regime.

3. Basic characteristics of the Vema Channel observations

Time series of (low-pass filtered) horizontal velocity vectors for the array (Fig. 5a) provide an unambiguous visualization of a flow regime dominated in the deepest

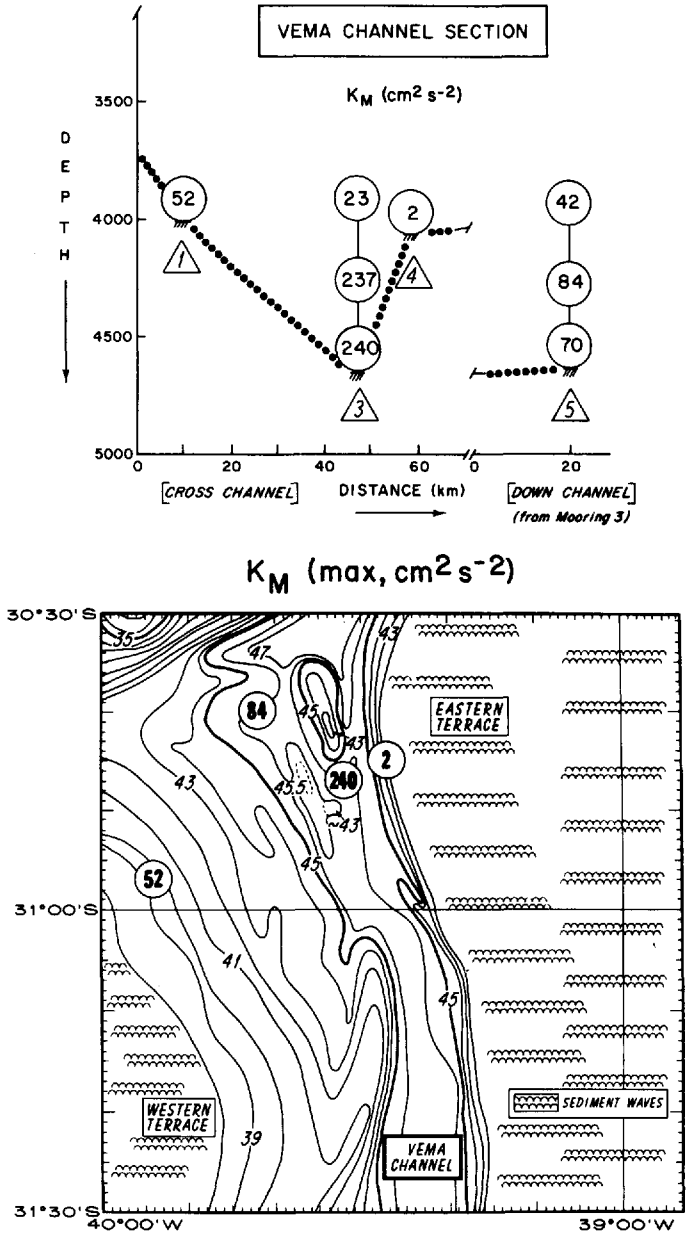

Figure 6. K_M summaries for Vema Channel (based on records from the second mooring setting, Table 2): (a) a section; (b) a map of maximum values. The section is a simplified version of Figure 4 and the map is a modification of Figure 2b, with site 2 deleted since there are no long-term data available there.

(central) part of Vema Channel, at moorings 688, 689, and 692, by a current that is typically large (~20 cm s^{-1} at 6893 and 6894) and persistently northward (or roughly along depth contours). The CTD data demonstrate that these sites are occupied at abyssal depths (below about 3700 m) by AABW (Hogg *et al.*, 1982). In the current at 6893 and 6894 there is only one interruption (southward flow) during the year of observation in Figure 5a, for a couple of weeks in July–August, 1981. This interruption is coherent vertically and by visual similarity also occurs nearly simultaneously (as a burst of flow with a southward component) at 6901, the closest mooring to 688. The currents at 6882 and 6883 were northward throughout. While comparatively persistent, the means at the lower two levels on 688 are smaller (by 50 to 75%) than those at comparable depths on 689, due presumably to less constricting topography at 689 (site 5; see Fig. 2 for channel geometry). It is also possible that these two moorings were simply located at different positions relative to a horizontally sheared flow, regardless of topographic detail. In contrast, 6881 is slightly larger in mean than 6891 and somewhat more persistent. 6924 is also notably stable in direction, and in fact has the biggest $\bar{v}$ near 4000 m depth (above the most constricting channel topography) for the entire array (larger even than 6881 and 6891, Table 2). 6901 is the one record clearly outside the current; v is negative, it is not in a northward flow like all the other meters, even though its water mass characteristics are also AABW (Hogg *et al.*, 1982). For frequencies containing 95% of K_E (periods greater than six days) 6893 and 6894 exhibit a coherence of .9 or larger (averaging over five basic frequency bands, so that a coherence above .73 is significant at the 95 percent level).

Moorings 688 and 689 exhibit the directionally steadiest (appearing) flows from the open ocean that we recall in addition 6893 and 6894 have the largest amplitude means. However, upon checking through the existing literature and data, we found two other (recent) observations of currents with similar properties, both in the vicinity of abyssal (thermohaline) flow regimes. These two locations are near the DWBC on the Blake-Bahama Outer Ridge (BBOR) and along the eastern foot of the Bermuda Rise. The former has been discussed by Jenkins and Rhines (1980) and Mills and Rhines (1979); the latter by Bird *et al.* (1982). Figure 5b is a time series of horizontal velocity vectors, in analogous format to Figure 5a, from an array of instruments deployed in the vicinity of the DWBC near the BBOR. Moorings 616, 617 and 618 were in the DWBC. There is a strong visual analogy between the time series of horizontal velocity vectors for mooring 618 (DWBC, BBOR, Fig. 5b) and 689 (AABW, Vema Channel, Fig. 5a), and record statistics (discussed below) are also similar.

K_M values in Table 2 vary from 2 to 240 $cm^2 s^{-2}$, generally dominated by $\overline{K}_v$. 240 $cm^2 s^{-2}$ is the largest mean kinetic energy that we are familiar with from any location in the world's abyssal ocean, slightly higher than the biggest values (~220 $cm^2 s^{-2}$) found in the DWBC along the Blake-Bahama Outer Ridge [see below; also, a mean flow (over eight months) of 22 cm s^{-1} (K_M ~ 240 $cm^2 s^{-2}$) has most recently been observed to flow roughly along depth contours at a height of 62 m up from the bottom along the

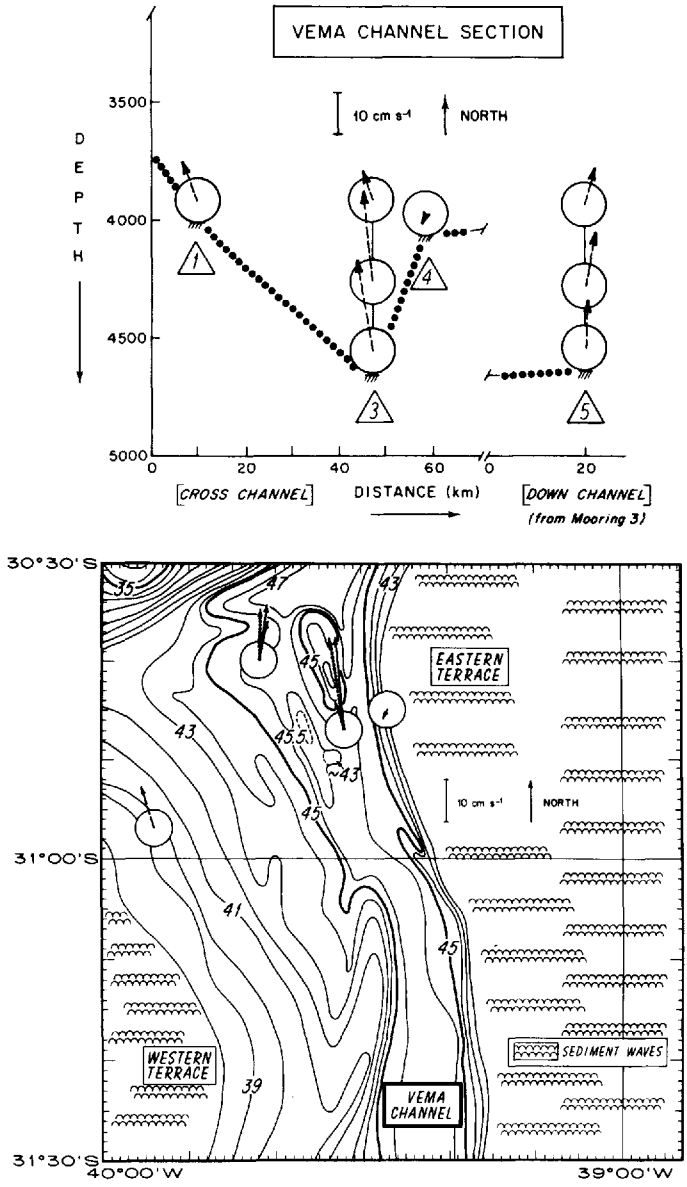

Figure 7. Time-averaged velocity vectors for Vema Channel (from the second mooring setting); in format analogous to that for Figure 6: (a) a section; (b) a map. Vectors from the vicinity of 4000 m depth are dashed; at mooring 688 and 689 those from the deepest level are dotted, intermediate levels are solid, reference Table 2.

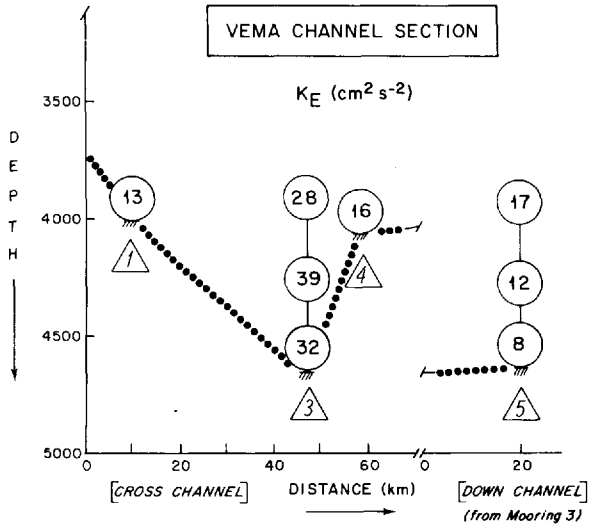

Figure 8. A section of K_E for Vema Channel.

eastward scarp of the Bermuda Rise (Bird *et al.*, 1982)]. K_M of 240 cm^2 s^{-2} occurs at the deepest mooring depths for site 3 (Fig. 6a), located near the axis and in the vicinity of a local constriction in Vema Channel (Figure 6b). In Figure 6a, K_M values are inserted into circles superimposed on an analogy to the section in Figure 4. Similarly, in Figure 6b, maximum K_M values for each mooring site are superimposed on a modified version of the map in Figure 2b. The location for mooring 2 is not entered on Figures 6a and 6b because there is no long-term data there (please note that this will be the case for all future figures of these types). The structure of the mean flow has been covered in detail by Hogg *et al.* (1982) and will not be considered further; the time-averaged vectors are shown for reference here in Figure 7.

K_E values for the Vema Channel current meter records (second setting) in Table 2 and Figure 8 vary from 8 to 39 cm^2 s^{-2}. The strongest mean flow ($K_M \sim 235$ to 240 cm^2 s^{-2}) and the strongest eddy field ($K_E \sim 32$ to 39 cm^2 s^{-2}) are both found at the same locations, at the two instruments moored nearest to the bottom on mooring 689 (site 3), near a constriction in the central segment of the deepest part of Vema Channel. Note that the complex topography just to the west of this site in Figure 2b (and 6b and 7b) is not well defined in detail by existing survey tracks (as suggested by the tentative way that these contours were entered on the figure). One might be tempted to associate the somewhat higher K_E at 6893 relative to 6894 (Table 2, Fig. 9) with the location of the former near the upper extension of the neighboring seamounts, whereas 6894 was located down between these topographic features. As another possibility, however, Hogg *et al.* (1982) show that isopycnals can reverse their slope toward the bottom within the channel, apparently in response to the constriction (Hogg, 1983b), pointing

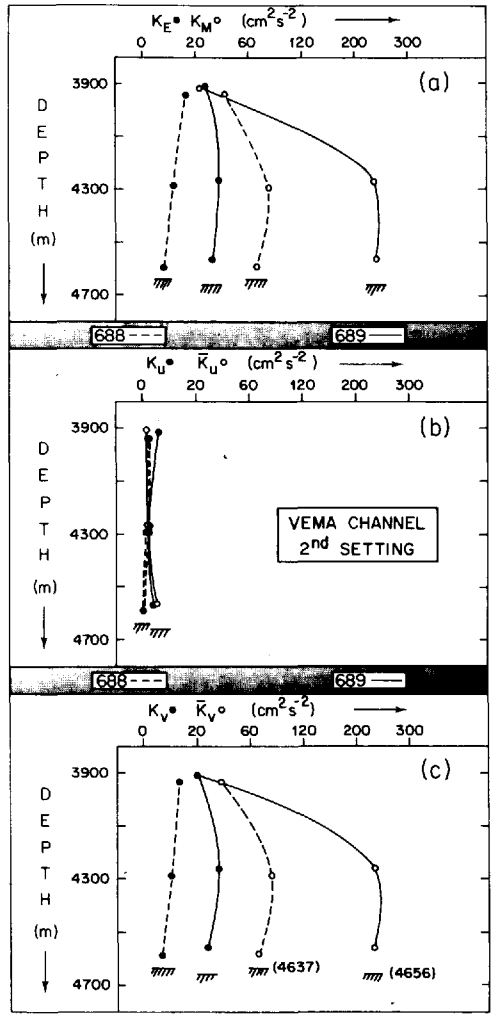

Figure 9. Vertical profiles of mean and eddy kinetic energy for the two more densely instrumented moorings (2nd setting) in Vema Channel: (a) total, (b) zonal, (c) meridional.

to a decrease in (geostrophic) velocity toward the bottom. The eddy field (Fig. 9) is predominantly meridional, roughly along depth contours, like the mean flow. K_E for 6893 (39 $cm^2 s^{-2}$) and 6894 (32 $cm^2 s^{-2}$) is nearly the same as K_E for 6183 (35 $cm^2 s^{-2}$), the latter record recently obtained from an analogous location (also having similar K_M, ~220 $cm^2 s^{-2}$) in the DWBC over the Blake-Bahama Outer Ridge.

Normalized distributions of K_E with frequency in Figure 10 indicate similar gross patterns for all levels at mooring 689, although there is some "bottom intensification"

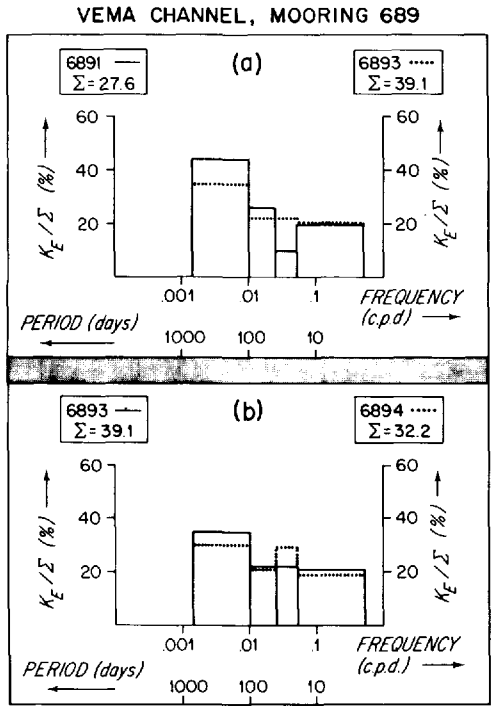

Figure 10. Frequency distributions for mooring 689, normalized (by Σ = total eddy kinetic energy).

in the 2 to 40 day range. However, the distributions of K_E for 6891 and 6924 are quite different in both amplitude (Fig. 11a) and pattern (Figure 11d), with 6924 containing much more relative energy in the highest (2 to 20 day) frequency band considered (50 versus 20%, note that 692 is over a much stronger local slope than 689). Neither 6901 or 6881 show much variability with frequency (Fig. 11b) for the band structure used. The major difference between 6891 and 6881 is for the lowest frequency band considered (Fig. 11c). In general, 689 records have a more energetic secular scale than 688, both dimensionally and normalized.

K_E (41.2, 700) for mooring 689 is not strongly depth-dependent (Fig. 12a), varying about a mid-point of around 19 by roughly ± 3 cm^2 s^{-2} only. K_E (2, 41.2) in Figure 12b is bottom intensified, increasing by a factor of roughly 2 from 6891 and 6893 and 6894. That is, at 689 the higher frequencies are bottom trapped while the lowest frequencies are weakly depth-dependent. Note, however, that the vertical variation of K_E (2, 41.2) at 689 is dominated by the vertical variation of K_E (20, 41.2; Fig. 12c) relative to that for K_E (2, 20; Fig. 12d). The latter result is in contrast to the case for the Ceara Rise data, see Section 4.

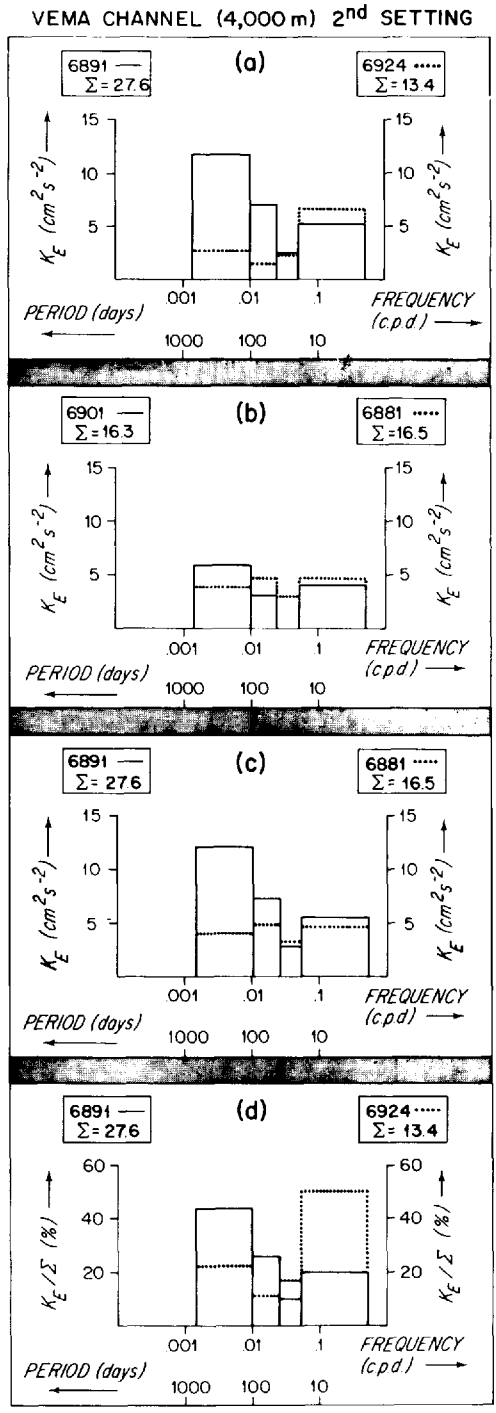

Figure 11. Frequency distributions for the Vema Channel 4000 m data. (d) is normalized by (Σ = total eddy kinetic energy) as in Figure 10.

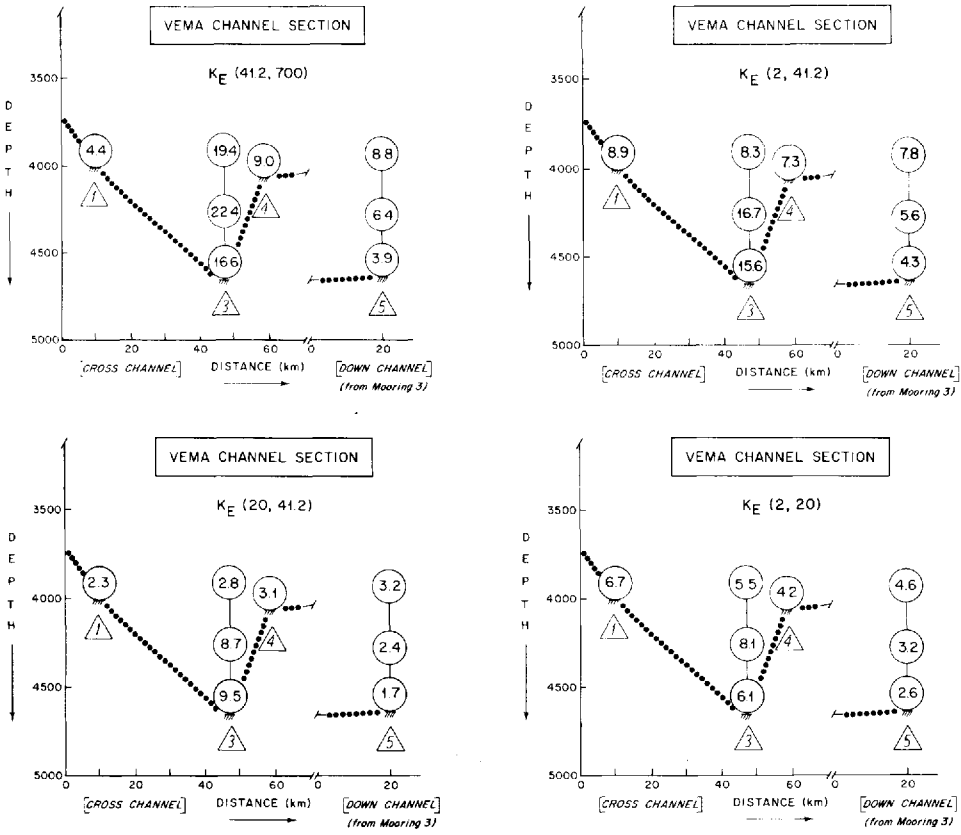

Figure 12. Sections of eddy kinetic energy (units $cm^2\ s^{-2}$) in a variety of period ranges: (a) K_E (41.2, 700); (b) K_E (2, 41.2); (c) K_E (20, 41.2); (d) K_E (2, 20).

Table 5. Frequency distribution of K_E for the Vema Channel and Blake-Bahama Outer Ridge. The period ranges for records of different lengths are dissimilar, as indicated in columns at each side of the Table.

Period ranges Blake-Bahama array (days)		K_E (6183)	K_E (6893)	K_E (6894)	K_E (AVG of 6893 + 6894)	Period ranges Vema Channel (days)	
T_1	T_2	($cm^2\ s^{-2}$)	($cm^2\ s^{-2}$)	($cm^2\ s^{-2}$)	($cm^2\ s^{-2}$)	T_1	T_2
2	19.4	7.4	8.1	6.1	7.1	2	20
19.4	40	7.9	8.7	9.5	9.1	20	41.2
40	97.2	13.2	8.6	6.8	7.7	41.2	100
97.2	680	6.7	13.8	9.8	11.8	100	700
Totals →		35.2	39.2	32.2	35.7	← Totals	

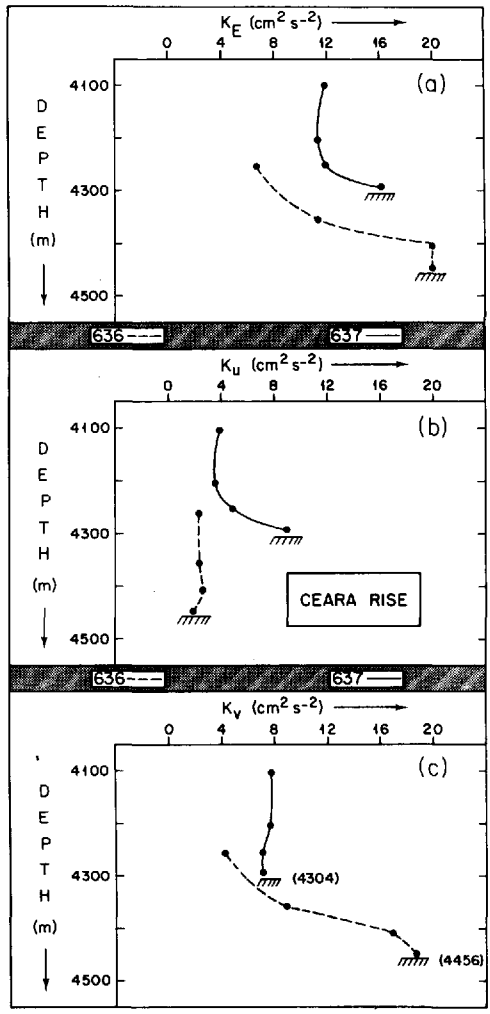

Figure 13. Vertical profiles of eddy kinetic energy for the Ceara Rise data: (a) total, (b) zonal, (c) meridional.

4. Comparison with data from other locations

The Vema Channel data may be compared with analogous observations from four moorings deployed for about a year in NADW over the Blake-Bahama Outer Ridge near 30N. The similarities between the DWBC array time series plots for low-passed horizontal velocity vectors (Fig. 5b) and the corresponding Vema Channel "stick plots" (Fig. 5a) have been noted in the first part of Section 3 above. This translates into similarities in record time-averages as well. Specifically (K_M, K_E) for 6893 and 6183 are (240, 39) and (220, 35), in cm^2 s^{-2}, respectively, very close indeed. However,

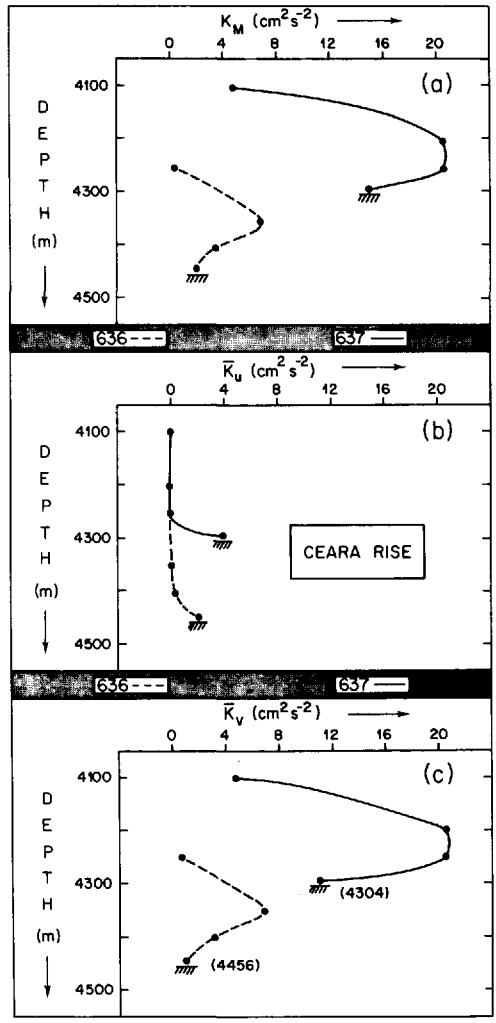

Figure 14. Vertical profiles of mean kinetic energy for the Ceara Rise data: (a) total, (b) zonal, (c) meridional.

frequency distributions for these records (Table 5) are somewhat different. K_E in the higher frequency bands is essentially the same, but the energy levels in the eddy and lowest frequency bands are interchanged between the two data sets. That is, K_E in the eddy band for the Vema records is roughly the same as K_E in the secular band for the DWBC records [and vice versa]. This difference is not dramatic; the variation is 7 to 14 cm^2 s^{-2} (Table 5). Another contrast between the two data sets is that the largest abyssal K_E for the BBOR data does not occur at the site with highest K_M (as is the case for Vema Channel). Rather, maximum K_E near 4000 m depth occurs at mooring 620

Table 6. Frequency distribution of K_E for the data from Vema Channel and the Ceara Rise. Period ranges where dissimilar, are indicated in columns at each side of the Table.

Period ranges Ceara Rise array (days)		K_E (6361)	K_E (6362)	K_E (6363)	K_E (6364)	K_E (6893)	Period ranges 2nd setting, Vema Channel (days)	
T_1	T_2	($cm^2 s^{-2}$)	($cm^2 s^{-2}$)	($cm^2 s^{-2}$)	($cm^2 s^{-2}$)	($cm^2 s^{-2}$)	T_1	T_2
2	20.6	2.6	5.3	12.0	14.0	8.1	2	20
20.6	42.4	.6	.7	1.1	1.0	8.7	20	41.2
42.4	103	2.2	3.9	5.1	4.0	8.6	41.2	100
103	720	1.3	1.4	1.3	.5	13.7	100	700
Totals →		6.7	11.3	19.5	19.5	39.1	← Totals	
20.6	720	4.1	6.0	7.5	5.5	31.0	20	700

near the foot of the BBOR ($K_E \sim 60$ cm^2 s^{-2} as compared to ~35 cm^2 s^{-2} in the current).

The Vema Channel results may also be examined in the context of observations from two moorings maintained for about a year in AABW in the vicinity of the Ceara Rise near 4N (Whitehead and Worthington, 1982). The high frequency content of this data set was discussed by Eriksen (1982). Current-temperature meters were deployed 10, 50, 100 and 200 m up from the sea floor (the bottom depths were 4304 m and 4456 m for moorings 636 and 637 respectively). Vertical profiles of K_E, K_u and K_v for the Ceara Rise data are contained in Figure 13; K_M, $\overline{K}_u$ and $\overline{K}_v$ are plotted in Figure 14. Bottom intensification of K_E in Figure 13 is rather strong for both Ceara Rise moorings, especially 636. The bottom intensification is essentially in K_v at 636; K_u is nearly depth-independent. For 637 the bottom intensification is predominantly associated with K_u; K_v hardly varies with depth. Frquency distributions for mooring 636 are listed and compared with 6893 in Table 6. The bottom intensification for 636 (similar remarks hold for 637) occurs primarily at the highest frequencies (periods of 2 to 20 days, Table 6); the depth dependence is weak (Table 6 for K_E (20, 720). In the eddy band the range of variation is roughly a factor of 2, whereas there is an order of magnitude difference at secular scales (Table 6). The Ceara Rise eddy field is about half as energetic as is the case in Vema Channel, or about 15% as energetic if contributions from periods less than about 20 days are not considered. The largest mean kinetic energy for the Ceara Rise data is about 5–10% of the largest Vema Channel value.

Three other regions are (briefly) compared with the Vema Channel results, either above or in the following section. At subtropical gyre latitudes we have the Gulf Stream abyssal data set and recent observations on the eastern scarp of the Bermuda Rise near the recirculation regime. The former has been recently summarized (in

conjunction with similar data from the western North Pacific) by Schmitz *et al.* (1982). The latter results were first published in the last year by Bird *et al.* (1982). The third data set was taken in the flow of NADW through the Charlie-Gibbs Fracture Zone (Schmitz and Hogg, 1978).

5. Summary and conclusions

An array of roughly year-long current meter records was recently deployed and recovered from the vicinity of Vema Channel, a major passage for the northward flow of AABW. Kinetic energies of the mean flow reached as high as 240 $cm^2\ s^{-2}$, and the intensity of the eddy field varied from 8 to 40 $cm^2\ s^{-2}$. The mean flow in Vema Channel is as energetic as ever observed in the abyssal ocean, although two other sites are now known to be comparable. These are located in the flow of North Atlantic Deep Water (in the DWBC) on the Blake-Bahama Outer Ridge, and along the eastern scarp of the Bermuda Rise. Abyssal eddy kinetic energy in the DWBC is also similar to that found at the Vema Channel site with the highest mean flow. Both mean flow and eddy intensity in the flow of AABW over the Ceara Rise (~4N) are roughly a factor of two lower than Vema Channel values. In the flow of NADW through the Charlie-Gibbs Fracture Zone at abyssal depths, K_M is a maximum of about 10 $cm^2\ s^{-2}$ and K_E about 20 $cm^2\ s^{-2}$ (Schmitz and Hogg, 1978).

Frequency distributions (normalized) have similar shapes at abyssal depths at mooring 689 in the center of Vema Channel (Fig. 10), but the higher frequencies (2 to 20 or 40 day periods) are more energetic near the edges of the passage. In contrast, secular scales are most energetic at mooring 689. K_E values for the mesoscale [taken (nominally) to be periods from 40 to 100 days for the data sets in question] in the thermohaline flow regimes examined (Vema Channel, Ceara Rise, NADW over the BBOR) are characteristically in the same range (~5 to 15 $cm^2\ s^{-2}$, say), roughly the same magnitude as analogous results from either the MODE area or from similar latitudes in the western North Pacific (Schmitz *et al.*, 1982). Higher frequencies (periods of 2 to 40 days) also exhibit similar intensity directly in the thermohaline flow regimes. However, these kinetic energies are larger than MODE or typical interior ocean values, a property seemingly characteristic of sites with topographic features.

Acknowledgments. We are grateful to the National Science Foundation for its support through grant numbers OCE78-25405 and OCE82-14255. Portions of the data analysis and manuscript preparation were made feasible by the Office of Naval Research under contract N00014-76-C-0197, NR 083-400. Dave Johnson kindly made his bathymetric results available prior to final publication. This is contribution number 5289 from the Woods Hole Oceanographic Institution.

REFERENCES

Bird, A. A., G. L. Weatherly and M. Wimbush. 1982. A study of the bottom boundary layer over the eastward scarp of the Bermuda Rise. J. Geophys. Res., *87*, 7941–7954.

Eriksen, C. C. 1982. Observations of internal wave reflection off sloping bottoms. J. Geophys. Res. *87,* 525–538.

Gould, W. J., W. J. Schmitz, Jr. and C. Wunsch. 1974. Preliminary field results for a Mid-Ocean Dynamics Experiment (MODE-0). Deep-Sea Res., *21,* 911–931.

Hogg, N. G. 1983a. A note on the deep circulation of the western North Atlantic: its nature and causes. Deep-Sea Res., *30,* (in press).

——1983b. Hydraulic control and flow separation in a multi-layered fluid with applications to the Vema Channel. J. Phys. Oceanogr., *13,* (in press).

Hogg, N. G., P. Biscaye, W. Gardner and W. J. Schmitz, Jr. 1982. On the transport and modification of Antarctic Bottom Water in the Vema Channel. J. Mar. Res., *40,* (Suppl.), 231–263.

Jenkins, W. J. and P. B. Rhines. 1980. Tritium in the deep North Atlantic Ocean. Nature, *286,* 877–880.

Johnson, D. A., S. E. McDowell, L. G. Sullivan and P. E. Biscaye. 1976. Abyssal hydrography, nephelometry, currents and benthic boundary layer structure in the Vema Channel. J. Geophys. Res., *81,* 5771–5786.

Mills, C. A. and P. Rhines. 1979. The deep western boundary current at the Blake-Bahama Outer Ridge: current meter and temperature observations, 1977–78. Woods Hole Oceanogr. Inst. Tech. Rept., W.H.O.I. Ref. No. 79–85.

Reid, J. L., W. D. Nowlin, Jr. and W. C. Patzert. 1977. On the characteristics and circulation of the Southwestern Atlantic Ocean. J. Phys. Oceanogr., *7,* 62–91.

Schmitz, W. J., Jr. 1974. Observations of low-frequency current fluctuations on the Continental Slope and Rise near Site D. J. Mar. Res., *32,* 233–251.

Schmitz, W. J., Jr. and N. G. Hogg. 1978. Observations of energetic low frequency current fluctuations in the Charlie-Gibbs Fracture Zone. J. Mar. Res. *36,* 725–734.

Schmitz, W. J., Jr., P. P. Niiler, R. L. Bernstein and W. R. Holland. 1982. Recent long-term moored instrument observations in the western North Pacific. J. Geophys. Res., *87,* 9425–9440.

Whitehead, J. A. and L. V. Worthington. 1982. The flux and mixing rates of Antarctic Bottom Water within the North Atlantic. J. Geophys. Res., *87,* 7903–7924.

Wyrtki, K., L. Magaard and J. Hager. 1976. Eddy energy in the Oceans. J. Geophys. Res., *81,* 2641–2646.

Received: *10 December, 1982;* revised: *13 April, 1983.*